Filtering Techniques for Chaotic Signals

*Chungyong Lee and *Douglas B. Williams

Abstract

Generalized iterative methods for reducing noise in contaminated chaotic signals are proposed. These methods minimize a cost function composed of two parts: one containing information that represents how close enhanced signals are to the observed signal and another composed of constraints that fit the dynamics of the system. The convergence conditions and the error systems of the proposed methods are investigated. As one aspect of noise reduction, the suppression or cancellation of a chaotic interference signal is discussed

I. Introduction

In many cases, the study of nonlinear dynamical systems and chaos has been motivated by the relationship between chaotic signals and random processes and has caused many researchers to reconsider what is meant by "noise". The deterministic signal from a nonlinear system may look like noise when displayed in either the time or frequency domain. Much of the engineering work in this area has involved a search for applications of these "noise-like" deterministic signals. For example, Cuomo and Oppenheim [6] have applied a chaotic system with the self-synchronization property to the secure communications problem. They have exploited the characteristics of the system to mask an information signal with the noise-like chaotic signal. However, for their implementation, if the level of additive noise due to the transmitting channel exceeds 10% of the driving signal, synchronization will not occur. Therefore, for their algorithm to succeed at low signal-to-noise ratios (SNRs), a noise reduction algorithm is necessary. Also, noise limits our ability to extract quantitative information from observed signals [8]. Obviously, noise reduction is essential for both the analysis and application of dynamical systems.

Unfortunately, conventional linear filtering methods cannot be applied successfully to signals produced by chaotic systems, because the signals have, generally, broad-band spectra. Moreover, a simple lowpass or bandpass filtering can change significantly the Lyapunov exponents and the fractal dimension of the reconstructed attractor [8]. To data, several methods [8], [9], [10], [11], [12] have been developed to remove noise from chaotic signals. These methods separate into two classes: those that assume the system dynamics are known and those that do not know the dynamics. Obviously, the latter case provides a robustness at the expense of performance. The choice of which method is suitable depends on the characteristics of application. For instance, in secure communication applications [6], [7] it is assumed that the dynamics of the system are known. In this paper we will consider the noise reduction methods which are applicable only when the system dynamics are known.

Farmer's method described by Farmer and Sidorowich [10] has nice performance in mild SNR circumstances. However, its structure is relatively complicated because it combines the manifold decomposition procedure and singular value decomposition for the inversion of a large rank deficient matrix. Therefore, we propose two classes of generalized iterative noise reduction schemes for contaminated chaotic signals which are simple and easily implemented. One class of these proposed methods estimates the deviation of the observed signal from the nearest noise-free signal and uses the result to get a noise-reduced signal. To calculate the deviation our techniques minimize a cost function composed of two parts: one containing information that represents how close the enhanced signals are to the observed signal and another composed of constraints that fit the dynamics of the system. Another class of these methods tries to enhance the observed signal by iteratively seeking the signal minimizing a cost function. Members of these classes vary as a result different choices for the parts of the cost function. We will show via numerical simulations that some versions of these schemes have better performance than Farmer's method for relatively low SNRs.

*Digital Signal Processing Laboratory School of Electrical and Computer Engineering Georgia Institute of Technology
Manuscript Received July 22, 1996.

II. Farmer's Method

Suppose that we have an M-dimensional nonlinear discrete-time dynamical system[1] described by a difference equation:

$$\mathbf{x}_{n+1} = f(\mathbf{x}_n), \quad n = 0, 1, 2, \cdots$$

where $\mathbf{x}_n \in R^M$ is the state vector point at time n and $f: R^M \mapsto R^M$ describes the dynamics of the system. The solution $\mathbf{x}_n$, $n = 0, 1, 2, \cdots$ of the difference equation is called an orbit. When the point $\mathbf{x}_n$ is contaminated with additive noise $\mathbf{x}_n$ and we observe the noisy point $\mathbf{y}_n = \mathbf{x}_n + \mathbf{w}_n$, our goal is to clean the noisy point $\mathbf{y}_n$ to estimate the noise-free point $\mathbf{x}_n$.

Farmer and Sidorowich [10] have used the Lagrange multiplier technique to minimize the cost function:

$$\sum_{n=0}^{N-1} \|\mathbf{y}_n - \hat{\mathbf{x}}_n\|^2 + 2 \sum_{n=0}^{N-2} \Lambda_n^T [f(\hat{\mathbf{x}}_n) - \hat{\mathbf{x}}_{n+1}],$$

where Λ_n indicates the Lagrange multipliers at time n, $\hat{\mathbf{x}}_n$ is an enhanced point, and N is the number of observed data points. If we define several variables: $\Delta_n \equiv \hat{\mathbf{x}}_n - \mathbf{x}_n$, $\Phi_n \equiv \mathbf{y}_n - \hat{\mathbf{x}}_{n+1}$, $\Upsilon_n \equiv \hat{\mathbf{x}}_{n+1} - f(\hat{\mathbf{x}}_n)$ and assume $\Lambda_n = 0$ for $n < 0$ or $n \geq N-1$, we can arrive at two linearized iterative equations to be solved by taking the derivatives of the cost function with respect to $\hat{\mathbf{x}}_n$ and Λ_n and setting them to zero. That is

$$\Phi_n = \mathbf{D} f(\hat{\mathbf{x}}_n)^T \Lambda_n - \Lambda_{n-1} - \Delta_n$$
$$\Delta_{n+1} = \mathbf{D} f(\hat{\mathbf{x}}_n) \Delta_n + \Upsilon_n,$$

where $\mathbf{D} f(\hat{\mathbf{x}}_n)$ is Jacobian of $f(\cdot)$ at $\hat{\mathbf{x}}_n$.

The above two equations can be cast into matrix form as follows:

$$\begin{bmatrix} -\mathbf{I} & \mathbf{D} f(\hat{\mathbf{x}}_0)^T & & & & & & \\ \mathbf{D} f(\hat{\mathbf{x}}_0) & \mathbf{0} & -\mathbf{I} & & & \mathbf{0} & & \\ & -\mathbf{I} & -\mathbf{I} & \mathbf{D} f(\hat{\mathbf{x}}_1)^T & & & & \\ & & \mathbf{D} f(\hat{\mathbf{x}}_1) & \mathbf{0} & -\mathbf{I} & & & \\ & & & \vdots & \vdots & \vdots & & \\ & \mathbf{0} & & & \mathbf{D} f(\hat{\mathbf{x}}_{N-2}) & \mathbf{0} & -\mathbf{I} \\ & & & & & -\mathbf{I} & -\mathbf{I} \end{bmatrix} \begin{bmatrix} \Delta_0 \\ \Lambda_0 \\ \Delta_1 \\ \Lambda_1 \\ \vdots \\ \Lambda_{N-2} \\ \Delta_{N-1} \end{bmatrix} = \begin{bmatrix} \Phi_0 \\ -\Upsilon_0 \\ \Phi_1 \\ -\Upsilon_1 \\ \vdots \\ -\Upsilon_{N-2} \\ \Phi_{N-1} \end{bmatrix}$$

and solved by inverting the matrix to get Δ_n, the deviation of the enhanced point from the true point. This approach works well for short trajectory segments, i.e., small N, but the matrix inversion can be computationally expensive. The so-called *manifold decomposition method* introduced by Hammel [9] is a fast and efficient technique that avoids this matrix inversion. It exploits the shadowing property of chaotic systems that a deterministic orbit can be found that is arbitrarily close to an observed noisy orbit [9], [10]. The noise reduction problem for a chaotic system can be viewed as seeking an approximation to the true orbit by finding the optimal shadowing orbit. The manifold decomposition method will be explained briefly.

If the trial solution $\hat{\mathbf{x}}$ would be complete (noise-free), then $\hat{\mathbf{x}}_n = f(\hat{\mathbf{x}}_{n-1})$. Let $\Phi_n = \mathbf{y}_n - \hat{\mathbf{x}}_n$ and $\Pi_n = f(\mathbf{y}_{n-1}) - \mathbf{y}_n$. Assuming $\hat{\mathbf{x}}_n$ is close to $\mathbf{y}_n$, we can get

$$\Phi_n \approx \mathbf{D} f(\hat{\mathbf{x}}_{n-1}) \Phi_{n-1} - \Pi_n \qquad (1)$$

For the two-dimensional case, if $\mathbf{e}_n$ and $\mathbf{c}_n$ are unit vectors in the expanding (unstable) and contracting (stable) directions, respectively, then Π_n and Φ_n can be decomposed into two directions.

$$\Pi_n = \zeta_n \mathbf{e}_n + \xi_n \mathbf{c}_n$$
$$\Phi_n = \alpha_n \mathbf{e}_n + \beta_n \mathbf{c}_n$$

For higher-dimensional cases, Π_n and Φ_n can be decomposed into stable and unstable subspaces. Since Π_n, $n = 0, \cdots, N-1$ can be calculated from N observed points, ζ_n and ξ_n, $n = 0, \cdots, N-1$ are easily obtained. Two iterative equations for α_n and β_n can be obtained by plugging the above two equations into (1) and considering for each direction

$$\alpha_n = \frac{\alpha_{n+1} + \zeta_{n+1}}{\|\mathbf{D} f(\hat{\mathbf{x}}_n) \mathbf{e}_n\|}, \quad \alpha_{N-1} = 0$$

$$\beta_{n+1} = \beta_n \|\mathbf{D} f(\hat{\mathbf{x}}_n) \mathbf{c}_n\| - \xi_{n+1}, \quad \beta_0 = 0.$$

[1] For convenience, only discrete-time dynamical systems are considered in this paper, though continuous-time dynamical systems may be treated in much the same manner.

Once we have α_n and β_n, we can calculate the deviation term Φ_n and then the estimated true point using Φ_n. Although the manifold decomposition method is fast, it is less accurate in the presence of homoclinic tangency [10], which occurs when the stable and unstable directions are nearly parallel. For points where homoclinic tangency occurs, Farmer and Sidorowich applied their Lagrange multiplier approach. However, homoclinic tangency may cause the matrix to be nearly rank deficient. In this case, the matrix inversion is accomplished by using Singular Value Decomposition (SVD).

Consequently, the manifold decomposition method and SVD are often combined such that the manifold decomposition method is used except for those points where homoclinic tangency occurs and SVD must be applied. However, combining the manifold decomposition procedure and SVD may be inconvenient when Farmer's method is applied to real systems, and SVD may require too much computation. Therefore, we suggest an iterative scheme for processing contaminated chaotic signals that has a simple structure.

III. Generalized Iterative Noise Reduction Methods

We will consider the noise removal process as a constrained optimization problem. Consequently, when we have a function $c_1(\hat{\mathbf{x}}, \mathbf{y})$ to be minimized with respect to $\hat{\mathbf{x}}_n$ under constraints $c_2(\hat{\mathbf{x}})=0$, a constrained cost function C can be defined using a weight function Γ (which could be a scalar or a matrix according to the form of $c_2(\cdot)$):

$$C=c_1(\hat{\mathbf{x}}, \mathbf{y})+\Gamma c_2(\hat{\mathbf{x}}). \tag{2}$$

The function $c_1(\cdot,\cdot)$ should measure the closeness between the enhanced points $\hat{\mathbf{x}}_n$ and the noisy points $\mathbf{y}_n$. The Euclidean distance between $\hat{\mathbf{x}}_n$ and $\mathbf{y}_n$ is an example of an acceptable $c_1(\cdot,\cdot)$. Alternatively, the correlation between $\hat{\mathbf{x}}_n$ and $\mathbf{y}_n$ is also a suitable choice for a $c_1(\cdot,\cdot)$, but it must be maximized instead of minimized. There exist many other candidates for $c_1(\cdot,\cdot)$.

The constraint function $c_2(\cdot)$ should be chosen to enforce the dynamics of the system. For example, if $f(\cdot)$ and $f^{-1}(\cdot)$ inidicate the forward dynamics and the backward (inverse) dynamics, respectively,

$$c_2(\hat{\mathbf{x}})=\sum_{n=L_1}^{N-L_1-1}\left\{\sum_{k=1}^{L_1}\|f^k(\hat{\mathbf{x}}_n)-\hat{\mathbf{x}}_{n+k}\|^2+\sum_{k=1}^{L_2}\|f^{-k}(\hat{\mathbf{x}}_n)-\hat{\mathbf{x}}_{n-k}\|^2\right\} \tag{3}$$

is one possible choice of $c_2(\cdot)$ for some positive integers L_1 and L_2, where $f^k(\cdot)$ and $f^{-k}(\cdot)$ indicate the k-fold composition of the forward dynamics $f(\cdot)$ and the backward dynamics $f^{-1}(\cdot)$, respectively, and N is the number of available data points. If $f^{-1}(\cdot)$ does not exist, the second term of (3) can be ignored.

Given $c_1(\cdot,\cdot)$ and $c_2(\cdot)$, we can find a solution by taking the derivatives of C with respect to $\hat{\mathbf{x}}_n$ and Γ, and setting them to zero.

$$\frac{\partial C}{\partial \hat{\mathbf{x}}_n}=\frac{\partial c_1(\hat{\mathbf{x}}, \mathbf{y})}{\partial \hat{\mathbf{x}}_n}+\Gamma\frac{\partial c_2(\hat{\mathbf{x}})}{\partial \hat{\mathbf{x}}_n}=0 \tag{4}$$

$$\frac{\partial C}{\partial \Gamma}=c_2(\hat{\mathbf{x}})=0 \tag{5}$$

We want to find $\hat{\mathbf{x}}_n$ satisfying both (4) and (5). In most cases, it is not easy to get a closed form solution because of the nonlinear terms in equations (4) and (5). However, we can estimate the deviation (noise) term or the solution iteratively.

The motivation for the proposed scheme stems from the so-called "iterative method" for solving the linear system $\mathbf{Ax}=\mathbf{b}$ [16]. When the amount of computation in solving $\mathbf{Ax}-\mathbf{b}=0$ is excessive, we may choose to settle for an approximation $\hat{\mathbf{x}}$, that can be obtained more quickly. In many cases, it is possible to develop an iterative method that, for any initial point, can produce an improved solution $\hat{\mathbf{x}}^{(i)}$ at the i-th iteration from the previous iteration's solution, $\hat{\mathbf{x}}^{(i-1)}$, that converges to $\mathbf{x}$ as the number of iterations increases. One common approach is to split the matrix $\mathbf{A}$. If $\mathbf{A}=\mathbf{A}_1-\mathbf{A}_2$, then the equation $\mathbf{Ax}-\mathbf{b}=0$ becomes $\mathbf{A}_1\mathbf{x}-\mathbf{A}_2\mathbf{x}-\mathbf{b}=0$. Therefore, we have the iterative scheme for solution:

$$\mathbf{A}_1\hat{\mathbf{x}}^{(i)}=\mathbf{A}_2\hat{\mathbf{x}}^{(i-1)}+\mathbf{b}. \tag{6}$$

This method requires that $\mathbf{A}_1$ should be a simple matrix to invert, such as a diagonal or triangular matrix. Also, the iterative method (6) converges for any starting point if and only if the magnitude of every eigenvalue of $\mathbf{A}_1^{-1}\mathbf{A}_2$ is less than 1.

A. Method I

Next, we apply this iterative approach to solving the nonlinear system of equations given in (4) and (5). When choosing suitable functions $c_1(\hat{\mathbf{x}}, \mathbf{y})$ and $c_2(\hat{\mathbf{x}})$ and constant Γ, we can arrange (4) in the following form

$$\hat{\mathbf{x}}_n-\mathbf{y}_n+h(\hat{\mathbf{x}}, \mathbf{y})=0 \tag{7}$$

for some nonlinear function $h(\cdot,\cdot)$. Since $\mathbf{y}_n = \mathbf{x}_n + \mathbf{w}_n$, under the assumption $\hat{\mathbf{x}}_n \approx \mathbf{x}_n$, equation (7) gives

$$\hat{\mathbf{w}}_n \approx h(\hat{\mathbf{x}}, \mathbf{y}). \tag{8}$$

Although $h(\hat{\mathbf{x}}, \mathbf{y})$ may contain $\hat{\mathbf{w}}_n$ terms as nonlinear components, we can assume that $\hat{\mathbf{w}}_n$ in equation (8) is an estimate of $\mathbf{w}_n$ should satisfy equation (8) as long as $\hat{\mathbf{x}}_n$ is son close to $\mathbf{x}_n$. Therefore, in the spirit of equation (6) for linear systems, we may estimate the noise (deviation) component using equation (8), and an enhanced point can be computed iteratively by setting $\hat{\mathbf{x}}_n^{(i)} \leftarrow \hat{\mathbf{x}}_n^{(i-1)} - \hat{\mathbf{w}}_n$ until the solution converges. Clearly, $\hat{\mathbf{w}}_n$ may not be a good estimate for the first several iterations, especially, when the SNR is very low. In those situations the terms in $\frac{\partial c_2(\hat{\mathbf{x}})}{\partial \hat{\mathbf{x}}_n}$ associated with the dynamical inconsistency of the noisy points may produce an unacceptably large correation term $\hat{\mathbf{w}}_n$ causing the solution $\hat{\mathbf{x}}_n$ to diverge. This behavior may be overcome by weighting the correction term $\hat{\mathbf{w}}_n$ with a constant K_1 according to a threshold δ.

$$\tilde{\mathbf{w}}_n = \begin{cases} K_1 \hat{\mathbf{w}}_n & \text{with } K_1 = 1 \quad \text{if } \|\hat{\mathbf{w}}_n\| \le \delta \\ K_1 \hat{\mathbf{w}}_n & \text{with } 0 < K_1 \ll 1 \quad \text{if } \|\hat{\mathbf{w}}_n\| > \delta \end{cases} \tag{9}$$

If zero-mean white Gaussian noise and an M-dimensional dynamical system are assumed, the $\|\hat{\mathbf{w}}_n\|^2$ possesses a χ^2 distribution with M degrees of freedom. Hence the probability density of $\|\hat{\mathbf{w}}_n\|^2$ can be calculated if we know the variance of the noise. Thus, using the distribution of $\|\hat{\mathbf{w}}_n\|^2$, a suitable δ may be found.

So, to estimate the enhanced data, we update each point in a manner analogous to equation (6)

$$\begin{aligned}\hat{\mathbf{x}}_n^{(i)} &= K_2 \hat{\mathbf{x}}_n^{(i,temp)} + (1-K_2)\hat{\mathbf{x}}_n^{(i-1)} \\ &= \hat{\mathbf{x}}_n^{(i-1)} - K_1 K_2 \hat{\mathbf{w}}_n^{(i)}\end{aligned} \tag{10}$$

$$\begin{aligned}\hat{\mathbf{x}}_n^{(i,temp)} &= \hat{\mathbf{x}}_n^{(i-1)} - K_1 \hat{\mathbf{w}}_n^{(i)} \\ \hat{\mathbf{w}}_n^{(i)} &= h(\hat{\mathbf{x}}_n^{(i-1)}, \mathbf{y})\end{aligned} \tag{11}$$

for a weighting constant $0 < K_2 \ll 1$. In these equations $\hat{\mathbf{x}}_n^{(i)}$ and $\hat{\mathbf{x}}_n^{(i-1)}$ are the enhanced points at the present i-th iteration and at the previous $(i-1)$-th iteration, respectively, as before. $\hat{\mathbf{x}}_n^{(i,temp)}$ is an intermediate enhanced point at the present i-th iteration using $h(\cdot,\cdot)$. Since K_2 is related to both the convergence speed and stability, it is efficient to set K_2 to a relatively small value for the first several iterations to guarantee stable convergence and then to use a relatively large value for later iterations to achieve faster convergence.

The iterative update scheme can be established as follows (Proposed Method I):

1. Initially set $\hat{\mathbf{x}}_n^{(0)} = \mathbf{y}_n$.
2. Estimate the deviation term $\hat{\mathbf{w}}_n$ using (11).
3. Weight the estimated deviation $\hat{\mathbf{w}}_n$ to avoid unacceptably large corrections using (9).
4. Computer a new point using (10).
5. Iterate steps 2-4 until convergence.

B. Method II

In Method I, we need to find suitable values for *two* weighting constants K_1 and K_2. This disadvantage can be alleviated by estimating the enhanced signal $\hat{\mathbf{x}}_n$ itself instead of the deviation term. We can arrange equation (4) with respect to $\hat{\mathbf{x}}_n$ including the "linear" terms to get the following for some nonlinear function $g(\cdot,\cdot)$

$$\hat{\mathbf{x}}_n = g(\hat{\mathbf{x}}, \mathbf{y}). \tag{12}$$

Since equation (12) must be satisfied whenever the enhanced point $\hat{\mathbf{x}}_n$ converges to the true point $\mathbf{x}_n$, we can estimate the enhanced point of the present iteration, $\hat{\mathbf{x}}_n^{(i)}$, by using $g(\hat{\mathbf{x}}^{(i-1)}, \mathbf{y})$. This result is based on the same concept as that behind equation (6). We can update a point using

$$\begin{aligned}\hat{\mathbf{x}}_n^{(i)} &= K_3 \hat{\mathbf{x}}_n^{(i,temp)} + (1-K_3)\hat{\mathbf{x}}_n^{(i-1)} \\ &= \hat{\mathbf{x}}_n^{(i-1)} + K_3\left[\hat{\mathbf{x}}_n^{(i,temp)} - \hat{\mathbf{x}}_n^{(i-1)}\right]\end{aligned} \tag{13}$$

$$\hat{\mathbf{x}}_n^{(i,temp)} = g(\hat{\mathbf{x}}^{(i-1)}, \mathbf{y}) \tag{14}$$

for a weighting constant $0 < K_3 \ll 1$. If we rearranged (4) with respect to the $\hat{\mathbf{x}}_n$ to include both "linear and nonlinear" terms, this method would tend to be unstable, since the nonlinear terms, in general, are very sensitive to noise and may make this iteration diverge[2]. Although the requirement in our original motivation suggested that the matrix $\mathbf{A}_1$ should be simple motivates the use of "linear" terms only in order to get equation (12), our investigations via numerical simulations show that this condition in most cases also results in stable convergence of this

[2] Let's consider the equation $x - y + xy + x^3 + 3x + y^3 = 0$. This equation can be arranged in several forms: for example, $x = \frac{1}{4}(y - xy - x^3 - y^3)$ or $x = \frac{1}{y+4}(y - x^3 - y^3)$. The former form would have better convergence characteristics than the latter form.

method.

The iterative update scheme can be established as follows (Proposed Method II):

1. Initially set $\hat{\mathbf{x}}_n^{(0)} = \mathbf{y}_n$.
2. Estimate an enhanced signal $\hat{\mathbf{x}}_n$ using (14).
3. Computer a new point using (13).
4. Iterate steps 2-3 until convergence.

Ⅳ. Examples

To get some insights, we will derive the key equations of the proposed methods I and II for a given cost function.

A. Example 1

In this example, we consider $c_1(\hat{\mathbf{x}}, \mathbf{y})$ to be the Euclidean distance between the enhanced points $\hat{\mathbf{x}}_n$ and the noisy points $\mathbf{y}_n$, $c_2(\cdot)$ to be given by (3), and the weight function $\Gamma = 1$. That is,

$$c_1(\hat{\mathbf{x}}, \mathbf{y}) = \sum_{n=0}^{N-1} \|\hat{\mathbf{x}}_n - \mathbf{y}_n\|^2$$

$$c_2(\hat{\mathbf{x}}) = \sum_{n=L_1}^{N-L_1-1} \left\{ \sum_{k=1}^{L_1} \|f^k(\hat{\mathbf{x}}_n) - \hat{\mathbf{x}}_{n+k}\|^2 + \sum_{k=1}^{L_2} \|f^{-k}(\hat{\mathbf{x}}_n) - \hat{\mathbf{x}}_{n-k}\|^2 \right\}.$$

For systems in which the inverse dynamics do not exist, the last term of $c_2(\hat{\mathbf{x}})$ may be ignored. However, in other cases it improves the performance of the method

If we take a derivative of C with respect to $\hat{\mathbf{x}}_n$ and set it to zero, then we get the following result, corresponding to equation (7).[3]

$$\begin{aligned} \hat{\mathbf{x}}_n - \mathbf{y}_n &+ \sum_{k=1}^{L_1} \mathbf{D}f^k(\hat{\mathbf{x}}_n)\left[f^k(\hat{\mathbf{x}}_n) - \hat{\mathbf{x}}_{n+k}\right] \\ &+ \sum_{k=1}^{L_2} \mathbf{D}f^{-k}(\hat{\mathbf{x}}_n)\left[f^{-k}(\hat{\mathbf{x}}_n) - \hat{\mathbf{x}}_{n-k}\right] \\ &- \sum_{k=1}^{L_1} \left[f^k(\hat{\mathbf{x}}_{n-k}) - \hat{\mathbf{x}}_n\right] \\ &- \sum_{k=1}^{L_2} \left[f^{-k}(\hat{\mathbf{x}}_{n+k}) - \hat{\mathbf{x}}_n\right] = 0, \end{aligned} \tag{15}$$

where $\mathbf{D}f^k(\cdot)$ and $\mathbf{D}f^{-k}(\cdot)$ are the products of the Jacobians of $f(\cdot)$ and $f^{-1}(\cdot)$, respectively, defined by

$$\mathbf{D}f^k(\hat{\mathbf{x}}_n) = \prod_{i=0}^{k-1} \mathbf{D}f(\hat{\mathbf{x}}_{n+i})$$

$$\mathbf{D}f^{-k}(\hat{\mathbf{x}}_n) = \prod_{i=0}^{k-1} \mathbf{D}f^{-1}(\hat{\mathbf{x}}_{n-i}).$$

Since $\mathbf{y}_n = \mathbf{x}_n + \mathbf{w}_n$, if the trial solution $\hat{\mathbf{x}}_n$ is close to $\mathbf{x}_n$, i. e., $\hat{\mathbf{x}}_n \approx \mathbf{x}_n$, then we have an equation for the deviation estimate corresponding to equation (11).

$$\begin{aligned} \hat{\mathbf{w}}_n \approx &\sum_{k=1}^{L_1} \mathbf{D}f^k(\hat{\mathbf{x}}_n)\left[f^k(\hat{\mathbf{x}}_n) - \hat{\mathbf{x}}_{n+k}\right] \\ &+ \sum_{k=1}^{L_2} \mathbf{D}f^{-k}(\hat{\mathbf{x}}_n)\left[f^{-k}(\hat{\mathbf{x}}_n) - \hat{\mathbf{x}}_{n-k}\right] \\ &- \sum_{k=1}^{L_1} \left[f^k(\hat{\mathbf{x}}_{n-k}) - \hat{\mathbf{x}}_n\right] - \sum_{k=1}^{L_2} \left[f^{-k}(\hat{\mathbf{x}}_{n+k}) - \hat{\mathbf{x}}_n\right] \end{aligned}$$

This deviation estimate does make sense when we consider the case when the enhanced point $\hat{\mathbf{x}}_n$ is converging to the true solution $\mathbf{x}_n$. If $\hat{\mathbf{x}}_n \approx \mathbf{x}_n$, the right hand side (RHS) of the above equation is nearly zero, resulting in only a small correction being made in the update equation (10). On the other hand, we can get an equation corresponding to equation (14) by re-arranging equation (15).

$$\begin{aligned} \hat{\mathbf{x}}_n = \frac{1}{1 + L_1 + L_2} &\left\{ \mathbf{y}_n - \sum_{k=1}^{L_1} \mathbf{D}f^k(\hat{\mathbf{x}}_n)\left[f^k(\hat{\mathbf{x}}_n) - \hat{\mathbf{x}}_{n+k}\right] \right. \\ &- \sum_{k=1}^{L_2} \mathbf{D}f^{-k}(\hat{\mathbf{x}}_n)\left[f^{-k}(\hat{\mathbf{x}}_n) - \hat{\mathbf{x}}_{n-k}\right] + \sum_{k=1}^{L_1} f^k(\hat{\mathbf{x}}_{n-k}) \\ &\left. + \sum_{k=1}^{L_2} f^{-k}(\hat{\mathbf{x}}_{n+k}) \right\} \end{aligned}$$

Similary, this signal estimator appears to work when we consider the RHS of the above equation under the assumption $\hat{\mathbf{x}}_n \approx \mathbf{x}_n$. In that case we can see from the update equation (13) that the correction term is approximately $\frac{K_3}{1 + L_1 + L_2} \mathbf{w}_n$ resulting in only a small correction. Therefore, we can guess that a smaller K_3 will give better performance. In Section V we will see, however, that a smaller value for K_3 slows the convergence.

Since noise (perturbation) components in an enhanced orbit $\hat{\mathbf{x}}$ may cause the $f^k(\cdot)$ and/or $f^{-k}(\cdot)$ terms to diverge with evolution, L_1 and L_2 should be small for low SNR cases, while larger L_1 and L_2 may be acceptable for high SNR cases. The determination of L_1 and L_2 is associated with the Lyapunov exponents of the system. To explain this, consider the two-dimensional Hénon map[4] with Lyapunov exponents $\lambda_1 = 0.42$ and $\lambda_2 = -1.62$. The rate of change of a state perturbation along the unstable direction is approximately proportional to $e^{\lambda_1 n}$ for forward evolution and $e^{-\lambda_2 n}$ for backward evolution. This relationship implies that the rate of change of a state per-

[3] Obviously, in this example, we cannot get the enhanced points for $n < L_2$ and $n > N - L_1 - 1$.

[4] The dynamics of the two-dimensional Hénon map are given in equation (25).

turbation for backward evolution is larger than for forward evolution. In order to get the same rate of change along both the stable and unstable directions, we must choose L_1 and L_2 such that

$$e^{L_1\lambda_1} \approx e^{-L_2\lambda_2}.$$

This condition implies that L_2 should be smaller than L_1 for the Hénon map when L_1 is chosen to guarantee stable convergence [17]. Obviously, choosing $L_1=1$ and $L_2=1$ is the safest way for stable convergence for low SNRs.

B. Example 2

In this example, we choose $c_1(\hat{\mathbf{x}}, \mathbf{y})$ associated with the correlation coefficient between the enhanced point $\hat{\mathbf{x}}_n$ and the noisy point $\mathbf{y}_n$ and $c_2(\hat{\mathbf{x}})$ as the simplest case of equation (3) with $L_1=1$, and the weight function $\Gamma=1$. The backward dynamics are not considered in this case, i.e., $L_2=0$. Thus

$$c_1(\hat{\mathbf{x}}, \mathbf{y}) = 1 - \frac{\sum_n \hat{\mathbf{x}}_n^T \mathbf{y}_n}{\sqrt{\sum_n \|\hat{\mathbf{x}}_n\|^2}\sqrt{\sum_n \|\mathbf{y}_n\|^2}}$$

$$c_2(\hat{\mathbf{x}}) = \sum_n \|f(\hat{\mathbf{x}}_n) - \hat{\mathbf{x}}_{n+1}\|^2.$$

When we compare this cost function with the cost function in Example 1, we observe that this cost function, in effect, weights $c_2(\cdot)$ by N.

Under the assumption that $\hat{\mathbf{x}}_n \approx \mathbf{x}_n$, we obtain an equation corresponding to equation (11):

$$\hat{\mathbf{w}}_n \approx 2\sqrt{m_x m_y}\ \mathbf{D}f(\hat{\mathbf{x}}_n)[f(\hat{\mathbf{x}}_n) - \hat{\mathbf{x}}_{n+1}] - 2\sqrt{m_x m_y}\ [f(\hat{\mathbf{x}}_{n-1}) - \hat{\mathbf{x}}_n] + \left(\frac{m_{xy}}{m_x} - 1\right)\hat{\mathbf{x}}_n, \qquad (16)$$

where $m_x = \sum_n \|\hat{\mathbf{x}}_n\|^2$, $m_y = \sum_n \|\mathbf{y}_n\|^2$, and $m_{xy} = \sum_n \hat{\mathbf{x}}_n^T \mathbf{y}_n$. Similarly, we can get an equation corresponding to equation (14).

$$\hat{\mathbf{x}}_n = \frac{m_x}{m_{xy} + 2m_x\sqrt{m_x m_y}}\ \{\mathbf{y}_n - 2\sqrt{m_x m_y}\ \mathbf{D}f(\hat{\mathbf{x}}_n)[f(\hat{\mathbf{x}}_n) - \hat{\mathbf{x}}_{n+1}] + 2\sqrt{m_x m_y}\ f(\hat{\mathbf{x}}_{n-1})\} \qquad (17)$$

When we investigate equation (16), assuming that the enhanced point is converging to the true solution, the RHS of equation (16) is close to zero because m_{xy} is, ideally, equivalent to m_x for large N. Thus, only a small correction, $K_1 K_2 \hat{\mathbf{w}}_n$, is performed in the update equation (10), giving validity to using equation (16) as a deviation estimator. Similarly, if the RHS of equation (17) is substituted into the update equation (13) under the assumption $\hat{\mathbf{x}}_n \approx \mathbf{x}_n$, only a small correction, approximately $\frac{K_3}{1+2\sqrt{m_x m_y}}\ \mathbf{w}_n$, is made.

V. Convergence Conditions

As with most discussions of convergence conditions, we will demonstrate requirements for local convergence with no guarantees of global convergence. However, from the results of the numerical experiments given in later section, we observe that even the local convergence achieved by these methods is relatively close to the true solution. Therefore, we will investigate the conditions on these methods that will guarantee local, but not necessarily global, convergence.

In is not easy to derive general formulas for $h(\cdot,\cdot)$, $g(\cdot,\cdot)$, K_1, K_2, and K_3 that guarantee convergence. However, by choosing K_1, K_2, and K_3 such that the deviation from the true solution at the i-th iteration is smaller than at the $(i-1)$-th one, we can have some confidence in convergence to the true solution. Thus, in order to get an upper bound on K_1, K_2, and K_3 for convergence, the following inequality should be solved with respect to these constants.

$$E\{\|\hat{\mathbf{x}}_n^{(i)} - \mathbf{x}_n\|^2 - \|\hat{\mathbf{x}}_n^{(i-1)} - \mathbf{x}_n\|^2\} < 0$$

Solution of this inequality using the knowledge of the system dynamics and the formula for expected values of higher moments is only straightforward for $i=1$, but this case is not sufficient to guarantee convergence.

Another criterion for the convergence of the proposed algorithms can be found by examining the conditions under which the correction term goes to zero with iterations. To determine these conditions we will consider a theorem associated to the stability of a system [13].

THEOREM 1: Given a dynamical system $\mathbf{x}_n = f(\mathbf{x}_{n-1})$ where $f(\mathbf{0}) = \mathbf{0}$ for all n, suppose there exists a scalar function $V(\mathbf{x}_n)$ such that $V(\mathbf{0}) = 0$ for all n, and

1. $V(\mathbf{x}_n)$ is positive definite for all n and all $\mathbf{x}_n \neq \mathbf{0}$;
2. $\Delta V(\mathbf{x}_n) = V(f(\mathbf{x}_n)) - V(\mathbf{x}_n) < 0$ for all n and all $\mathbf{x}_n \neq \mathbf{0}$,

then the equilibrium state (origin) is equiasymptotically stable and $V(\mathbf{x}_n)$ is a Lyapunov function of the system.

In order to see whether the correction term goes to zero with iterations, we need to see whether the origin of the correction system is stable. To investigate it, we consider the energy function as a Lyapunov function candidate[5] for the correction system

$$V(\mathbf{x}_n) = \|\mathbf{x}_n\|^2 = \hat{\mathbf{x}}_n^T \mathbf{x}_n. \tag{18}$$

First, let's consider the correction system associated with proposed Method I. From the update equation (10), if the correction term $\hat{\mathbf{w}}_n^{(i)} \to 0$ as $i \to \infty$, then $\hat{\mathbf{x}}_n^{(i)} = \hat{\mathbf{x}}_n^{(i-1)}$, implying that $\hat{\mathbf{x}}_n^{(i)}$ converges. Therefore, if we can find a condition on K_1K_2 guaranteeing $\hat{\mathbf{w}}_n^{(i)} = h(\hat{\mathbf{x}}^{(i-1)}, \mathbf{y}) \to 0$ as $i \to \infty$, it would serve as a guideline for choosing K_1K_2. Using equations (10) and (11) and the Taylor series approximation for $h(\hat{\mathbf{x}}^{(i)}, \mathbf{y})$[6], we can get the following correction system for the method corresponding to equation (11).

$$\begin{aligned}
\hat{\mathbf{w}}_n^{(i+1)} &= h(\hat{\mathbf{x}}^{(i)}) \\
&= h\left(\hat{\mathbf{x}}^{(i)} - K_1K_2\, h(\hat{\mathbf{x}}^{(i-1)})\right) \\
&\approx \left[\mathbf{I} - K_1K_2\, \mathbf{D}h(\hat{\mathbf{x}}^{(i-1)})\right] h(\hat{\mathbf{x}}^{(i-1)}) \\
&= \prod_{k=0}^{i-1} \left[\mathbf{I} - K_1K_2\, \mathbf{D}h(\hat{\mathbf{x}}^{(i-k-1)})\right] h(\hat{\mathbf{x}}^{(0)}) \\
&= \prod_{k=0}^{i-1} \left[\mathbf{I} - K_1K_2\, \mathbf{D}h(\hat{\mathbf{x}}^{(i-k-1)})\right] \hat{\mathbf{w}}_n^{(1)} \\
&= \prod_{k=0}^{i-1} \mathbf{C}_1^{(i-k-1)}\, \hat{\mathbf{w}}_n^{(1)},
\end{aligned} \tag{19}$$

where $\mathbf{D}h(\hat{\mathbf{x}}^{(k)})$ is the Jacobian of $h(\cdot,\cdot)$ at $\hat{\mathbf{x}}^{(k)}$. To investigate the stability of the origin of the correction system given by equation (19), let's apply the stability theorem to the Lyapunov function candidate in equation (18). Then, we obtain the following result.

$$\begin{aligned}
\Delta V\left(h(\hat{\mathbf{x}}^{(i)})\right) &= V\left(\left[\mathbf{I} - K_1K_2\mathbf{D}h(\hat{\mathbf{x}}^{(i)})\right] h(\hat{\mathbf{x}}^{(i)})\right) - V\left(h(\hat{\mathbf{x}}^{(i)})\right) \\
&= \left\| \left[\mathbf{I} - K_1K_2\mathbf{D}h(\hat{\mathbf{x}}^{(i)})\right] h(\hat{\mathbf{x}}^{(i)}) \right\|^2 - \|h(\hat{\mathbf{x}}^{(i)})\|^2 \\
&= h(\hat{\mathbf{x}}^{(i)})^T \left\{ \left[\mathbf{I} - K_1K_2\mathbf{D}h(\hat{\mathbf{x}}^{(i)})\right]^T \right. \\
&\qquad \left. \left[\mathbf{I} - K_1K_2\mathbf{D}h(\hat{\mathbf{x}}^{(i)})\right] - \mathbf{I} \right\} h(\hat{\mathbf{x}}^{(i)}) \\
&= h(\hat{\mathbf{x}}^{(i)})^T \left\{ \mathbf{C}_1^{(i)T}\mathbf{C}_1^{(i)} - \mathbf{I} \right\} h(\hat{\mathbf{x}}^{(i)})
\end{aligned} \tag{20}$$

From the theorem, if $\Delta V\left(h(\hat{\mathbf{x}}^{(i)})\right) < 0$, the origin of the correction system is stable and this algorithm is convergent. Therefore, we see that this algorithm will converge if $\mathbf{C}_1^{(i)T}\mathbf{C}_1^{(i)} - \mathbf{I}$ is negative definite for all i.[7] Since the convergence matrix contains K_1K_2, we can get convergence conditions by choosing K_1K_2 such that $\mathbf{C}_1^{(i)T}\mathbf{C}_1^{(i)} - \mathbf{I}$ is negative definite. However, we cannot get a closed form expression for the convergence conditions on K_1K_2 to make $\mathbf{C}_1^{(i)T}\mathbf{C}_1^{(i)} - \mathbf{I}$ negative definite, since $\mathbf{D}h(\cdot,\cdot)$ is generally asymmetric and all possible $\hat{\mathbf{x}}^{(i)}$ must be considered.

Therefore, by investigating the largest singular value of $\prod_{k=0}^{i-1}\mathbf{C}_1^{(i-k-1)}$ in equation (19) as $i \to \infty$ we suggest a "numerical criterion" for determining both an *approximate range* on the weighting constants K_1, K_2, and K_3 *and* whether the selected nonlinear functions $h(\cdot,\cdot)$ and $g(\cdot,\cdot)$ are suitable for noise reduction purposes. If the largest singular value $\prod_{k=0}^{i-1}\mathbf{C}_1^{(i-k-1)}$ approaches zero as $i \to \infty$, we see that $\hat{\mathbf{w}}_n^{(i)} \to 0$ from equation (19) and the algorithm is convergent. Therefore, this route can be used to acquire the information needed for the convergence of the algorithm. Unfortunately, the product of the convergence matrices is difficult to calculate because the system evolves along the iteration index i instead of along the time index n and we do not know $\hat{\mathbf{x}}_n^{(i)}$ for all i a priori. However, we propose to calculate the range of K_1K_2 for which the largest singular value of the product of the convergence matrices approaches zero along the noisy orbit $\mathbf{y}_n$. We expect this range to give suitable information for convergence, because $\mathbf{C}_1^{(i)}$ can be regarded as a sequence of *random matrices* whose elements have finite mean and variance, and the growth rate of the system given in equation (19) is bounded by the largest singular value of some matrices of the sequence [15].

Figure 1 shows an experimental result for the largest singular value of the product of convergence matrices in equation (19) for the two-dimensional Hénon map after applying the algorithm for 200 iterations for various K_1K_2. The SNR was 10 dB. From this experiment, we can see that the suitable range for convergence is approximately between 0.0003 and 0.0014. The lower bound of $K_1K_2 = 0.0003$ comes from the following fact: if $K_1K_2 \approx 0$, $\hat{\mathbf{w}}_n^{(i)} \approx \hat{\mathbf{w}}_n^{(1)}$ from

[5] This energy function is considered frequently for many physical systems. However, this Lyapunov function candidate is not suitable for determining the stability of *every* physical system. Nonetheless, if we can show the existence of a Lyapunov function for the given correction system, the exact convergence conditions can be described by determining the ranges of the weighting constants and proper $h(\cdot,\cdot)$ and $g(\cdot,\cdot)$ that satisfy $\Delta V < 0$.

[6] We assume that $K_1K_2\,h(\hat{\mathbf{x}}^{(i-1)}, \mathbf{y})$ is small enough that higher order terms in the Taylor series expansion can be neglected. If this is not true, the result may be unreliable. To simplify our notation, we will not show the y term in $h(\hat{\mathbf{x}}^{(i)}, \mathbf{y})$.

[7] We will call $\mathbf{C}_1^{(i)}$ a "convergence matrix".

equation (19) implying no convergence. Figure 2 represents the change of the largest singular value with iteration for various K_1K_2. The same situation is assumed as for Figure 1. We can see that the largest singular value approaches zero when K_1K_2 lies in the appropriate range for convergence.

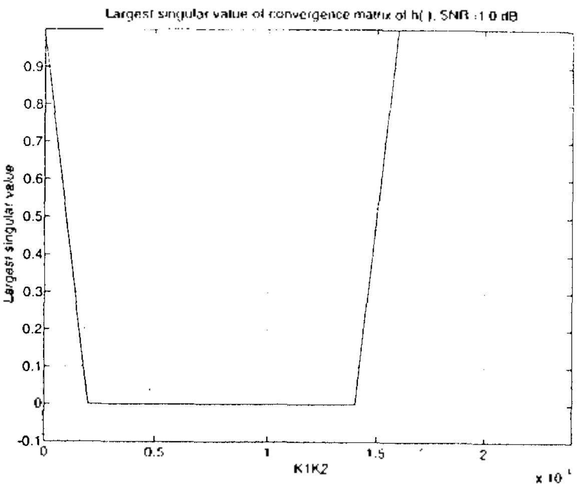

Figure 1. The largest singular value of $\prod_{k=0}^{i-1} C_i^{(i-k-1)}$ for the two-dimensional Hénon map with various K_1K_2 after 200 iterations. The SNR is 10 dB.

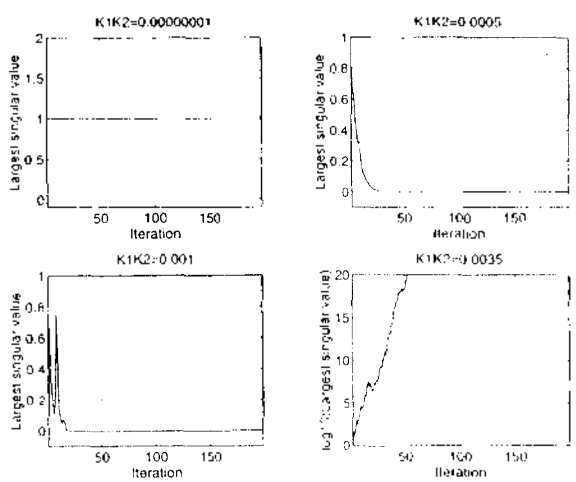

Figure 2. Change in the largest singular value for the two-dimensional Hénon map with iteration for various K_1K_2. The SNR is 10 dB. For the case $K_1K_2 = 0.0035$, the system diverged.

On the other hand, since the growth rate of the system given in equation (19) is closely related to the Lyapunov exponents of the system[*] $\hat{x}^{(i)} - K_1K_2h(\hat{x}^{(i)})$, we claim that if the convergence system has all negative Lyapunov exponents, the origin of the correction system is asymptotically stable and the algorithm is convergent. By regarding $\hat{w}^{(1)}$ in equation (19) as an initial perturbation, we see that the value of $\hat{w}^{(i)}$ as $i \to \infty$ is independent of the initial perturbation, if the convergence system has all negative Lyapunov exponents. Therefore, we can get an approximate range on suitable values of K_1K_2 by finding those K_1K_2 for which all the Lyapunov exponents of the convergence system are negative. If there exist no values of K_1K_2 for which all the Lyapunov exponents of the convergence system are negative, we must consider another form of $h(\cdot,\cdot)$. As before, we propose to calculate the range of K_1K_2 for which all the Lyapunov exponents of the convergence system are negative along the noisy orbit $\mathbf{y}_n$.

Figure 3 shows an experimental result for the estimated Lyapunov exponents of the convergence system for the two-dimensional Hénon map for various choices of K_1K_2 and SNR. We applied the method described in [5] to estimate the Lyapunov exponents. One Lyapunov exponent appears to be negative for all K_1K_2 and SNRs. However, the other Lyapunov exponent is not always negative. Obviously, the results for a SNR of 10 dB is very similar to the results in Figure 1.

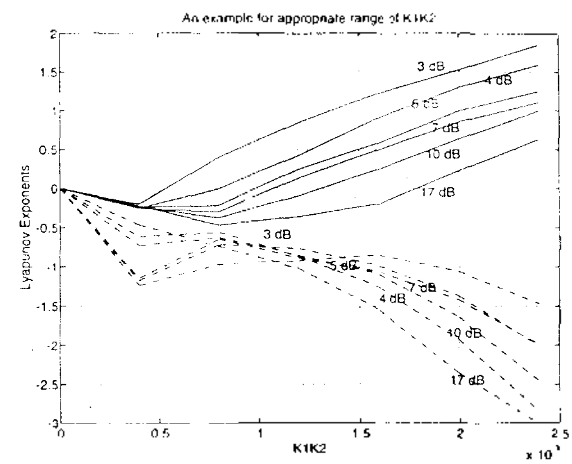

Figure 3. The estimated Lyapunov exponents of the convergence system of equation (16) for the two-dimensional Hénon map for various K_1K_2 and SNRs. One Lyapunov exponent is plotted with a solid a solid line and other with a dashed line. The method described in [5] was applied to estimate the Lyapunov exponents. The SNRs are 17, 10, 7, 5, 4, and 3 dB and $N = 200$.

Next, let's consider the system corresponding to proposed Method II. To get an approximate range for K_3 in

* We will call this type of system a "convergence system".

the same manner as before, we find the convergence system of $g(\cdot,\cdot)$ and observe all the Lyapunov exponents of the convergence system. From equation (13), if a correction system given by $\tilde{\mathbf{e}}_n^{(i)} \equiv \tilde{\mathbf{x}}_n^{(i,temp)} - \hat{\mathbf{x}}_n^{(i-1)} \rightarrow 0$ as $i \rightarrow \infty$, the algorithm will converge. We consider the following equations obtained using equation (13) and the Taylor series expansion.

$$\begin{aligned}\tilde{\mathbf{e}}_n^{(i)} &\equiv \tilde{\mathbf{x}}_n^{(i,temp)} - \hat{\mathbf{x}}_n^{(i-1)} \\ &= g\left(\hat{\mathbf{x}}^{(i-2)} + K_3 \tilde{\mathbf{e}}^{(i-1)}\right) - \hat{\mathbf{x}}_n^{(i-1)} \\ &\approx g(\hat{\mathbf{x}}^{(i-2)}) - \hat{\mathbf{x}}^{(i-1)} + K_3 \mathbf{D}g(\hat{\mathbf{x}}^{(i-2)})\tilde{\mathbf{e}}^{(i-1)} \\ &= \left[(1-K_3)\mathbf{I} + K_3 \mathbf{D}g(\hat{\mathbf{x}}^{(i-2)})\right] \tilde{\mathbf{e}}_n^{(i-1)} \\ &= \prod_{k=2}^{i} \left[(1-K_3)\mathbf{I} + K_3 \mathbf{D}g(\hat{\mathbf{x}}^{(i-k)})\right] \tilde{\mathbf{e}}_n^{(1)} \\ &= \prod_{k=2}^{i} \mathbf{C}_2^{(i-k)} \tilde{\mathbf{e}}_n^{(1)} \qquad (21)\end{aligned}$$

If the origin of the correction system $\tilde{\mathbf{e}}_n^{(i)}$ is stable, then $\tilde{\mathbf{e}}_n^{(i)} \rightarrow 0$ as $i \rightarrow \infty$ implying convergence of this method. Similary, recalling the stability theorem and the Lyapunov function candidate in equation (18), we can derive a convergence condition for this algorithm.

$$\begin{aligned}\Delta V\left(\tilde{\mathbf{e}}_n^{(i)}\right) &= V\left(\left[(1-K_3)\mathbf{I} + K_3 \mathbf{D}g(\hat{\mathbf{x}}^{(i-1)})\right] \tilde{\mathbf{e}}_n^{(i)}\right) - V\left(\tilde{\mathbf{e}}_n^{(i)}\right) \\ &= \left\| \left[(1-K_3)\mathbf{I} + K_3 \mathbf{D}g(\hat{\mathbf{x}}^{(i-1)})\right] \tilde{\mathbf{e}}_n^{(i)} \right\|^2 - \left\| \tilde{\mathbf{e}}_n^{(i)} \right\|^2 \\ &= \tilde{\mathbf{e}}_n^{(i)T} \left\{ \left[(1-K_3)\mathbf{I} + K_3 \mathbf{D}g(\hat{\mathbf{x}}^{(i-1)})\right]^T \right. \\ &\qquad \left. \left[(1-K_3)\mathbf{I} + K_3 \mathbf{D}g(\hat{\mathbf{x}}^{(i-1)})\right] - \mathbf{I} \right\} \tilde{\mathbf{e}}_n^{(i)} \\ &= \tilde{\mathbf{e}}_n^{(i)T} \left\{ \mathbf{C}_2^{(i-1)T} \mathbf{C}_2^{(i-1)} - \mathbf{I} \right\} \tilde{\mathbf{e}}_n^{(i)} \qquad (22)\end{aligned}$$

As before, if $\Delta V\left(\tilde{\mathbf{e}}_n^{(i)}\right) < 0$, then this method is convergent. Therefore, we have the convergence condition that requires the matrix $\mathbf{C}_2^{(i)T}\mathbf{C}_2^{(i)} - \mathbf{I}$ to be negative definite for all i. As before, we cannot get exact closed form conditions of K_3 and $g(\cdot,\cdot)$ such that this condition is met for all $\hat{\mathbf{x}}^{(i)}$.

Therefore, we consider the convergence system of this algorithm to get an approximate range on K_3 and $g(\cdot,\cdot)$. In this case, the convergence system is $(1-K_3)\hat{\mathbf{x}}_n^{(i)} + K_3 g(\hat{\mathbf{x}}^{(i)})$. If the convergence system has all negative Lyapunov exponents, $\tilde{\mathbf{e}}_n^{(i)}$ should converge to the origin as $i \rightarrow \infty$. As before, we can get an approximate range for K_3 by identifying those values of K_3 that allow all the Lyapunov exponents of the convergence system to be negative. If there exists no upper limit on K_3 for which all the Lyapunov exponents of the convergence system are negative, we must try another form of $g(\cdot,\cdot)$. Figure 4 shows an experimental result for the Lyapunov exponents of the convergence system of equation (17) for the two-dimensional Hénon map according to various K_3 and SNR. These Lyapunov exponents were also estimated by applying the method in [4].

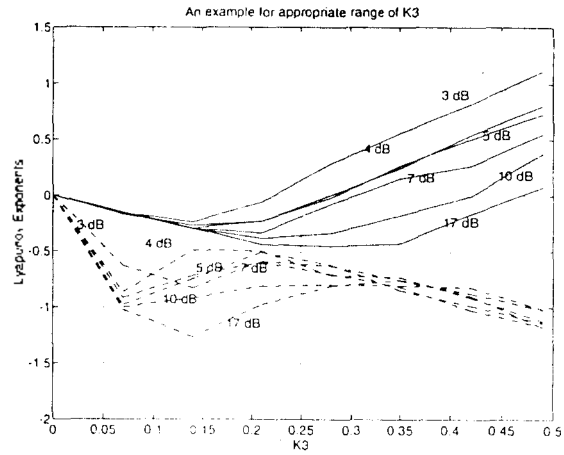

Figure 4. The estimated Lyapunov exponents of the convergence system of equation (17) for the two-dimensional Hénon map for various K_3 and SNRs. One Lyapunov exponent is plotted with a solid line and other with a dashed line. The method described in [5] was applied to estimate the Lyapunov exponents. The SNRs are 17, 10, 7, 5, 4, and 3 dB and $N = 200$.

Ⅵ. Error Systems

In this section we will observe the steady state behavior of the error system of the proposed methods under the assumption that the correction system has a stable origin. To see what happens to the proposed methods with iterations, we will define an error system as the difference between the true point and the enhanced point at the i-th iteration, i.e., $\hat{\mathbf{e}}_n^{(i)} = \mathbf{x}_n - \hat{\mathbf{x}}_n^{(i)}$.

First, consider proposed Method I. Using the update equation (10), equation (19), and the Taylor series expansion, we can derive the following equations.

$$\begin{aligned}\hat{\mathbf{e}}_n^{(i)} &= \mathbf{x}_n - \hat{\mathbf{x}}_n^{(i)} \\ &= \hat{\mathbf{e}}_n^{(i-1)} + K_1 K_2\, h(\hat{\mathbf{x}}^{(i-1)}) \\ &= \hat{\mathbf{e}}_n^{(0)} + K_1 K_2 \sum_{k=0}^{i-1} h(\hat{\mathbf{x}}^{(i-k-1)}) \\ &= -\mathbf{w}_n + K_1 K_2 \sum_{k=0}^{i-1} h(\hat{\mathbf{x}}^{(i-k-1)})\end{aligned}$$

$$\approx -\mathbf{w}_n + K_1K_2 \sum_{k=0}^{i-1} \left\{ \prod_{j=0}^{i-k-2} \left[\mathbf{I} - K_1K_2\mathbf{D}h(\hat{\mathbf{x}}^{(i-k-j-2)}) \right] h(\hat{\mathbf{x}}^{(0)}) \right\}$$

$$\approx -\mathbf{w}_n + K_1K_2 \sum_{k=0}^{i-1} \left\{ \prod_{j=0}^{i-k-2} \left[\mathbf{I} - K_1K_2\mathbf{D}h(\hat{\mathbf{x}}^{(i-k-j-2)}) \right] \mathbf{D}h(\mathbf{x}) \right\} \mathbf{w}_n \qquad (23)$$

where we use the facts that $\hat{\mathbf{x}}_n^{(0)} = \mathbf{y}_n = \mathbf{x}_n + \mathbf{w}_n$ and, for the true orbit $\mathbf{x}$, $h(\mathbf{x}) \approx 0$ as explained before. We observe that the second term of the RHS of equation (23) is the sum of linear combinations of $\mathbf{w}_n$, and, if the origin of the correction system is stable, only a limited number of terms are present in the sum. However, it is not easy to show analytically that the sum converges to $\mathbf{w}_n$.

Second, consider the proposed Method II and its error system $\hat{\mathbf{e}}_n^{(i)}$ defined as before. In this case we see the steady state behavior of the error system more clearly. From equation (13), we have the following result:

$$\begin{aligned}\hat{\mathbf{e}}_n^{(i)} &\equiv \mathbf{x}_n - \hat{\mathbf{x}}_n^{(i)} \\ &= \mathbf{x}_n - \left[K_3 \hat{\mathbf{x}}_n^{(i,\,temp)} + (1-K_3)\hat{\mathbf{x}}_n^{(i-1)} \right] \\ &= (1-K_3)\hat{\mathbf{e}}_n^{(i-1)} + K_3 \tilde{\mathbf{e}}_n^{(i)},\end{aligned}$$

where $\tilde{\mathbf{e}}_n^{(i)} \equiv \mathbf{x}_n - \hat{\mathbf{x}}_n^{(i,\,temp)}$. Iterating the above equation with respect to $\hat{\mathbf{e}}_n^{(0)}$ and recalling that $\hat{\mathbf{e}}_n^{(0)} = \mathbf{x}_n - \hat{\mathbf{x}}_n^{(0)} = \mathbf{x}_n - \mathbf{y}_n$, we get

$$\begin{aligned}\hat{\mathbf{e}}_n^{(i)} &= (1-K_3)^i \hat{\mathbf{e}}_n^{(0)} + \sum_{k=0}^{i-1} K_3(1-K_3)^k \tilde{\mathbf{e}}_n^{(i-k)} \\ &= -(1-K_3)^i \mathbf{w}_n + \sum_{k=0}^{i-1} K_3(1-K_3)^k \tilde{\mathbf{e}}_n^{(i-k)} \qquad (24)\end{aligned}$$

From equation (24), we see that $\hat{\mathbf{e}}_n^{(i)} \approx 0$ as $i \to \infty$ if we choose K_3 as small as possible because the initial error terms cannot affect the whole error system as $i \to \infty$ due to the scale factor $(1-K_3)^k$. On the other hand, it may be more efficient to select K_3 to be close to 1 for fast convergence due to the term $(1-K_3)^i$. However, as shown in Figure 4, K_3 should be small enough to guarantee all negative Lyapunov exponents for the convergence system. Therefore, we can see that there exists a trade-off between fast convergence and stable convergence.

VI. Separation of Chaotic Information Signals

In this seciton, we will consider a separation technique for mixed chaotic signals that can also be used as a cancellation technique for chaotic interference signals. Signal separation or cancellation can also be regarded as a noise filtering problem. Chaotic signal separation and cancellation is necessary when we consider the smart jamming and multipath situations affecting the secure communications techniques using chaotic systems [19]

A. Augmented Dynamical Systems

When we observe a (vector) sequence $\mathbf{v}_n$ that is the mixed version of the sequences $\mathbf{x}_n^1$, $\mathbf{x}_n^2$, $\cdots$, $\mathbf{x}_n^L$ from L chaotic systems and all system dynamics f_1, f_2, $\cdots$, f_L are known, the noise removal problem is to recover $\mathbf{x}_n^1$, $\mathbf{x}_n^2$, $\cdots$, $\mathbf{x}_n^L$ from $\mathbf{v}_n = c_1\mathbf{x}_n^1 + c_2\mathbf{x}_n^2 + \cdots + c_L\mathbf{x}_n^L + \mathbf{w}_n$, where $\mathbf{w}_n$ is white Gaussian noise. From these assumptions, we can see that the signal separation problem is the same as the state estimation problem of the following "augmented" dynamical system.

$$\begin{aligned}\mathbf{z}_{n+1} &= F(\mathbf{z}_n) \\ \mathbf{v}_n &= \mathbf{c}\mathbf{z}_n + \mathbf{w}_n, \end{aligned} \qquad (25)$$

where $\mathbf{z}_n$ and $F(\cdot)$ are augmented state vector and augmented system dynamics, respectively, defined by

$$\mathbf{z}_n = \begin{bmatrix} \mathbf{x}_n^1 \\ \mathbf{x}_n^2 \\ \vdots \\ \mathbf{x}_n^L \end{bmatrix}$$

$$F(\mathbf{z}_n) = \begin{bmatrix} f_1(\mathbf{x}_n^1) \\ f_2(\mathbf{x}_n^2) \\ \vdots \\ f_L(\mathbf{x}_n^L) \end{bmatrix}$$

and $\mathbf{c}$ a row vector defined by $\mathbf{c} = [c_1\ c_2\ \cdots\ c_L]$ for constant values c_i, $i = 1, 2, \cdots, L$. To estimate $\mathbf{z}_n$, we will consider two approaches: the augmented extended Kalman filter approach and the augmented iterative noise reduction approach.

B. Augmented Extended Kalman Filter Approach

The Kalman filter has been designed to estimate the state vector in a linear dynamical model. If the model is nonlinear, a linearization procedure is usually performed resulting in the so-called extended Kalman filter(EKF) [14].

When an augmented dynamical system (25) is constructed from the observed sequence $\mathbf{v}_n$ and knowledge of the system dynamics f_i, $i = 1, 2, \cdots, L$, the nonlinear model (25) is approximated by the linear model obtained using the linear Taylor approximation of $F(\mathbf{z}_n)$ at a predicted state vector $\hat{\mathbf{z}}_n$:

$$F(\mathbf{z}_n) \approx F(\hat{\mathbf{z}}_n) + \mathbf{D}F(\hat{\mathbf{z}}_n)(\mathbf{z}_n - \hat{\mathbf{z}}_n),$$

where $\mathbf{D}F(\mathbf{z}_n)$ is the Jacobian matrix of $F(\cdot)$ at $\mathbf{z}_n$. When formulate $\hat{\mathbf{z}}_n \equiv \hat{\mathbf{z}}_{n|n}$ using the predicted state vectors

$$\hat{\mathbf{z}}_{n+1|n} = F(\hat{\mathbf{z}}_n),$$

we can get a (approximated) linear dynamical model

$$\begin{aligned} \mathbf{z}_{n+1} &= \mathbf{D}F(\hat{\mathbf{z}}_n)\mathbf{z}_n + \mathbf{u}_n \\ \mathbf{v}_n &= \mathbf{c}\mathbf{z}_n + \mathbf{w}_n, \end{aligned} \tag{26}$$

where $\mathbf{u}_n = F(\hat{\mathbf{z}}_n) - \mathbf{D}F(\hat{\mathbf{z}}_n)\hat{\mathbf{z}}_n$. This linearization is useful only if $\hat{\mathbf{z}}_0$ has been determined and, in most cases, $\hat{\mathbf{z}}_0 = E\{\mathbf{z}_0\}$. From the Kalman filtering results for a linear model, we get the correction formula

$$\hat{\mathbf{z}}_n = \hat{\mathbf{z}}_{n|n-1} + \mathbf{G}_n(\mathbf{v}_n - \mathbf{c}\hat{\mathbf{z}}_{n|n-1}),$$

where $\mathbf{G}_n$ is the Kalman gain matrix for the linear model (26) at the n-th instant. The resulting filtering process is called the EKF for an augmented system (25).

The filtering algorithm may be summarized as follows:
Initial conditions:

- $\mathbf{P}_{0,0} = Var\{\mathbf{z}_n\}$
- $\hat{\mathbf{z}}_0 = E\{\mathbf{z}_0\}$

For $n = 1, 2, 3, \cdots$

- $\mathbf{P}_{n,n-1} = \mathbf{D}F(\hat{\mathbf{z}}_{n-1})\mathbf{P}_{n-1,n-1}\mathbf{D}F(\hat{\mathbf{z}}_{n-1})^T$
- $\hat{\mathbf{z}}_{n|n-1} = F(\hat{\mathbf{z}}_{n-1})$
- $\mathbf{R}_n = Var\{\mathbf{w}_n\}$
- $\mathbf{G}_n = \mathbf{P}_{n,n-1}\mathbf{c}^T(\mathbf{c}\mathbf{P}_{n,n-1}\mathbf{c}^T + \mathbf{R}_n)^{-1}$
- $\mathbf{P}_{n,n} = (\mathbf{I} - \mathbf{G}_n\mathbf{c})\mathbf{P}_{n,n-1}$
- $\hat{\mathbf{z}}_n = \hat{\mathbf{z}}_{n|n-1} + \mathbf{G}_n(\mathbf{v}_n - \mathbf{c}\hat{\mathbf{z}}_{n|n-1})$

By appling the above algorithm, we can estimate the augmented state vector $\mathbf{z}_n$ to get $\mathbf{x}_n^1, \mathbf{x}_n^2, \cdots, \mathbf{x}_n^L$.

C. Augmented Iterative Noise Reduction Approach

We can treat the chaotic signal separation problem in the framework of the generalized iterative noise reduction method described in the previous sections, whenever the observed sequence is cast into the form of the augmented dynamical system given by equation (25). If the augmented system (25) is given, a natural and simple approach is to find the enhanced point $\hat{\mathbf{z}}_n$ that minimizes the following cost function:

$$C = \sum_n \|\mathbf{v}_n - \mathbf{c}\hat{\mathbf{z}}_n\|^2 + \sum_n \|\hat{\mathbf{z}}_{n+1} - F(\hat{\mathbf{z}}_n)\|^2. \tag{27}$$

From the condition $\frac{\partial C}{\partial \hat{\mathbf{z}}_n} = 0$, we can get an equation defining the estimate $\hat{\mathbf{z}}_n$. For example,

$$\hat{\mathbf{z}}_n = (\mathbf{v}_n - \mathbf{c}\hat{\mathbf{z}}_n)\mathbf{c}^T + F(\hat{\mathbf{z}}_{n-1}) + \mathbf{D}F(\hat{\mathbf{z}}_n)(\hat{\mathbf{z}}_{n+1} - F(\hat{\mathbf{z}}_n)).$$

If the above equation satisfies the convergence conditions mentioned in Section V, we can estimate the augmented $\mathbf{z}_n$ by applying Method II proposed in Section III-B. This approach is simpler than the augmented EKF approach. However, this approach has a weak point in that it does not use the knowledge of the system dynamics f_i, $i = 1, 2, \cdots, L$ "interactively" while it tries to find the signal that is close to a $\mathbf{v}_n$ that is corrupted by other signals. This is clear when we oberve that $\mathbf{D}F(\cdot)$ is a block diagonal matrix. On the other hand, this approach can be considered within the framework of the generalized iterative noise reduction method and can be applied to general situations, as can the augmented EKF approach.

D. On Concellation of Chaotic Interference Signals

For the chaotic signal separation problem, it is not always possible to have all the information about the system dynamics f_i, $i = 1, 2, \cdots, L$. In may smart smart jamming scenarios, the system dynamics for the jamming signals are not available. Since want to remove the jamming signals without any knowledge of their system dynamics, we will consider the cancellation instead of the separation of these chaotic interference signals.

When we observe $\mathbf{v}_n$ composed of an information signal $\mathbf{x}_n^1$ generated by the given system with dynamics f_1, the interference signals, and additive noise, and want to extract $\mathbf{x}_n^1$, the only viable approach is to treat the jamming signals as noise and apply a noise reduction method using the system dynamics f_1. One issue in applying a noise reduction method that uses system dynamics is how to select an "initial solution" that avoids local minima. Because an interference signal with a dominant mean value can move the initial solution $\mathbf{v}_n$ away from the true solution, an interference signal with a mean value far away from the mean value of the information signal $\mathbf{x}_n^1$ may lead the solution to local minimum if we choose the observed signal $\mathbf{v}_n$ itself as initial solution. Therefore, from our experience with the interference cancellation problem, we recommend setting the initial solution as follows:

$$v_n = \frac{1}{N}\sum_{n=0}^{N-1} v_n + E\{x_n^1\} \quad (28)$$

where $E\{x_n^1\}$ can be calculated by using the knowledge f_1. In summary, we may remove the interference signals by applying a noise reduction method that uses the system dynamics with the initial solution given by equation (28).

Ⅶ. Numerical Experiments

For the noise reduction problem, the performance of the proposed noise reduction Methods I and II is compared with that of Farmer's method for white Gaussian noise. The sensitivity of the proposed noise reduction methods to the homoclinic tangency problem is investigated. For the problem of chaotic signal separation, the performance of the augmented EKF approach and the augmented iterative noise reduction approach is investigated. Also, for the problem of chaotic interference cancellation, the effect of the selection of the initial solution is demonstrated. The performance is discussed from two viewpoints: that of the true error and that of the dynamical error. The true error is defined as the difference between the noise free-point x_n and the enhanced point $\hat{x}_n$:

$$e_{1,n} = \hat{x}_n - x_n. \quad (29)$$

The dynamical error is defined as the inconsistency of the dynamics of the enhanced data $\hat{x}_n$:

$$e_{2,n} = \hat{x}_n - f(\hat{x}_{n-1}). \quad (30)$$

A. White Gaussian Noise Case

In this section noise reduction results are presented for the two-dimensional Hénon map [1] which is governed by

$$x_{1,n+1} = 1 - 1.4x_{1,n}^2 + x_{2,n}$$
$$x_{2,n+1} = 0.3x_{1,n}. \quad (31)$$

Figure 5 shows the mean squared error (MSE) for each coordinate of the true error and the dynamical error according to various SNRs after Farmer's method, the proposed Method I, and the proposed Method II are applied to anoisy two-dimensioanl Hénon map. In both cases we used the cost functions described in Section IV-*B*. The proposed Method I was iterated for 200 times with $K_1=0.06667$ and $K_2=0.003$, while the proposed Method II was iterated for 200 time $K_3=0.08$. Farmer's method was iterated for 20 times. The corrupting noise was additive white Gaussian noise. The proposed methods have shown better performance than Farmer's method with regards to both the true error and the dynamical error. Also, the proposed Method II is more convenient than the proposed Method I since it requires only one weighting constant K_3. Though the proposed scheme requires more iterations than Farmer's method, it still requires fewer computations than Farmer's method. Moreover, its structure is much simpler because it does not require the matrix inversion or SVD calculation required by Farmer's method. From this result, we can that the proposed methods have better performance at *relatively low SNRs*[9] than Farmer's method.

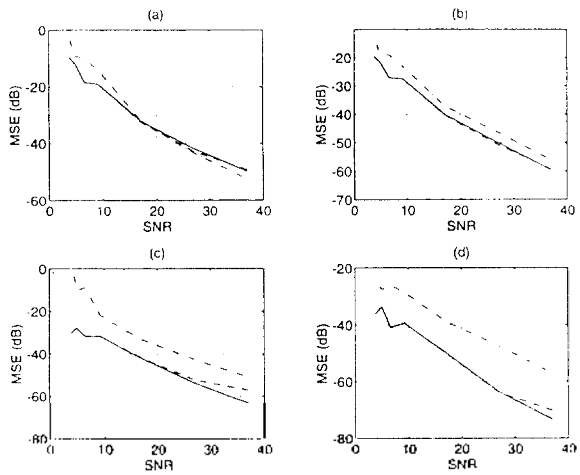

Figure 5. The mean squared errors for Farmer's method (dash-dotten), proposed Method I (dashed), and proposed Method II (solid) for the Hénon map according to various NRs. The subfigures depict (a) the true error for the first coordinate, (b) the true error for the second coordinate, (c) the dynamical error for the first coordinate, and (d) the dynamical error for the second coordinate.

Figure 6 compares the sensitivity of proposed noise reduction Method I to the homoclinic tangency problem with that of Farmer's method. Farmer's method and the proposed Method I were applied to the noisy two-dimensinal Hénon signal with a SNR of 8 dB. The first subfigure depicts the logarithm of the estimated angle between the

[9] In high SNR cases, for example over 20 dB, we observed that Farmer's method shows better performance in the true error of the first coordinate of the two-dimensional Hénon map. However, our goal is a method with good performance at low SNRs to be applied to applications of chaotic systems.

stable and unstable directions at each point. Therefore, the instances with small values indicate where the stable direction and the unstable direction are nearly parallel, i.e., homoclinic tangency points. The second and third subfigures show the first and second, respectively, coordinates of the true error after applying Farmer's method. In the forth and fifth subfigures the first and second, respectively, coordinates of the true error after applying the proposed Method I are shown. Clearly, we can see that the proposed method is less sensitive to the homoclinic tangency problem that Farmer's method.

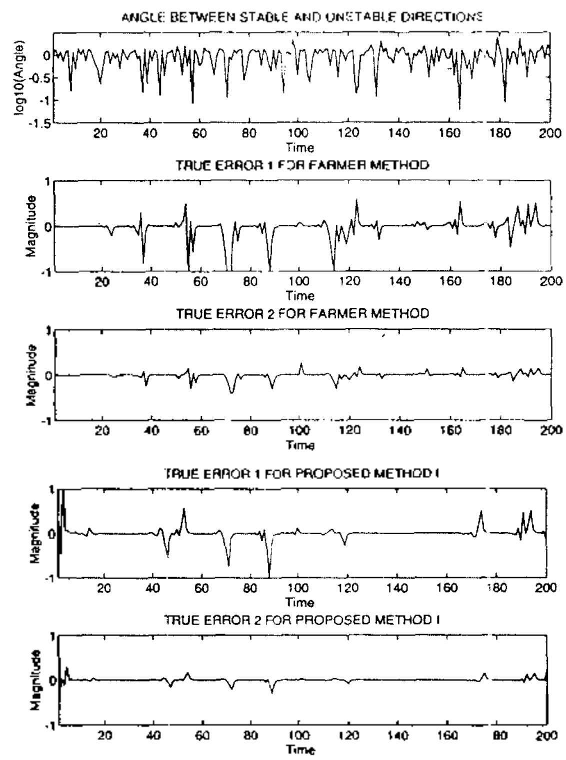

Figure 6. The sensitivity of Farmer's method and the proposed Method I to the homoclinic tangency problem. The first subfigure depicts the logarithm of the estimated angle between the stable and unstable directions at each point. The second and third subfigures show the first and second, respectively, coordinates of the true error after applying Farmer's method. The forth and fifth subfigures indicate the first and second, respectively, coordinates of the true error after applying the proposed Method I.

B. Chaotic Interference Signal Case

In this section, the results for chaotic interence signal separation are shown. We assume that a signal from the one-dimensional Hénon map described by

$$x^1_{n+1} = 1 - 1.4(x^1_n)^2 + 0.3x^1_{n-1}$$

is corrupted by a signal from the one-dimensional Logistic map governed by

$$x^2_{n+1} = 3.7x^2_n(1 - x^2_n)$$

and white Gaussina noise w_n. We observe the signal $v_n = x^1_n + x^2_n + w_n$ and want to separate x^1_n and x^2_n from v_n. We indicate SNR_i is the signal-to-noise ratio between signal $\mathbf{x}^i_n$ and noise $\mathbf{w}_n$. The signal to interference signal ratio, SIR_{ij}, is defined by

$$\mathrm{SIR}_{ij} = 10\log_{10}\left(\frac{\frac{1}{N}\sum_{n=0}^{N-1}\|\mathbf{x}^i_n - \bar{\mathbf{x}}^i_n\|^2}{\frac{1}{N}\sum_{n=0}^{N-1}\|\mathbf{x}^j_n - \bar{\mathbf{x}}^j_n\|^2}\right), \tag{32}$$

where $\bar{\mathbf{x}}^i_n = \frac{1}{N}\sum_{n=0}^{N-1}\mathbf{x}^i_n$ and N is the number of data samples.

Figure 7 shows the MSE of the ture error and the dynamical error for each signal according to the various SNR_i's. For these simulations $\mathbf{c} = [1\ \ 1]$ and SIR_{12} was 11 dB. For the results of the augmented EKF approach, the errors generated during transients are ignored in calculating

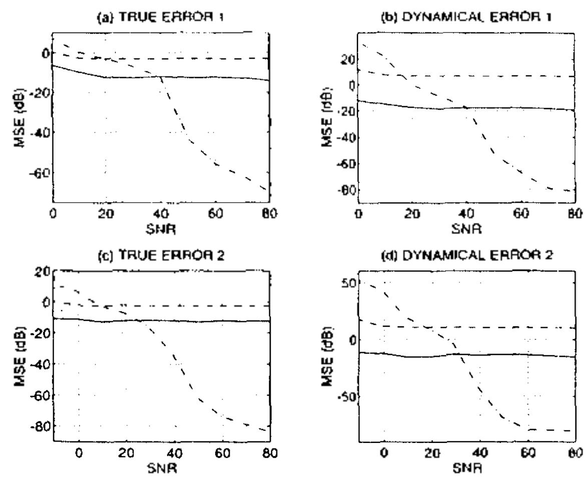

Figure 7. The mean squared errors of the original signal (dashed), the augmented EKF approach (dash-dotted), and the augmented iterative noise reduction approach (solid) according to various SNRs. subfigures depict (a) the true error for the Hénon map, (b) the dynamical error for the Hénon map, (c) the true error for the Logistic map, and (d) the dynamical error for the Logistic map. $\mathrm{SIR}_{12} = 11$ dB. For the augmented EKF approach the errors generated during transient time are ignored.

[10] Grassberger's method is not described in this paper. Refer to [12] for algorithm.

the MSE. for both types of errors, we can observe that the augmented EKF approach gives good results at relatively high SNR_i while it is sensitive to even a small amount of noise. On the other hand, the augmented iterative noise reduction approach seems to be insensitive to the noise but does not improve significantly for high SNR_i's. In conclusion, the applications of both approaches may be limited because the augmented EKF requires high SNRs (over 40 dB) and the iterative noise reduction approach shows poor overall performance.

C. Effects Due to the Initial Solution

In this section, the effects of the selection of the initial solution for interference signal cancellation are demonstrated. We assume that the information signal is the one-dimensional Hénon signal and that we know the dynamics of the information signal. The Logistic signal is used as an interference signal, and no knowledge of the dynamics of the interference signal is assumed. The additive noise is white Gaussian noise with a 10 dB SNR_I. SNR_{I2} was 11 dB. To remove the Logistic interference signal, we applied Grassberger's method [12][10] and the proposed noise reduction Method II for two cases : case 1 assumes that the initial is the observed signal itself and case 2 uses the initial solution with equation (28). Each method was

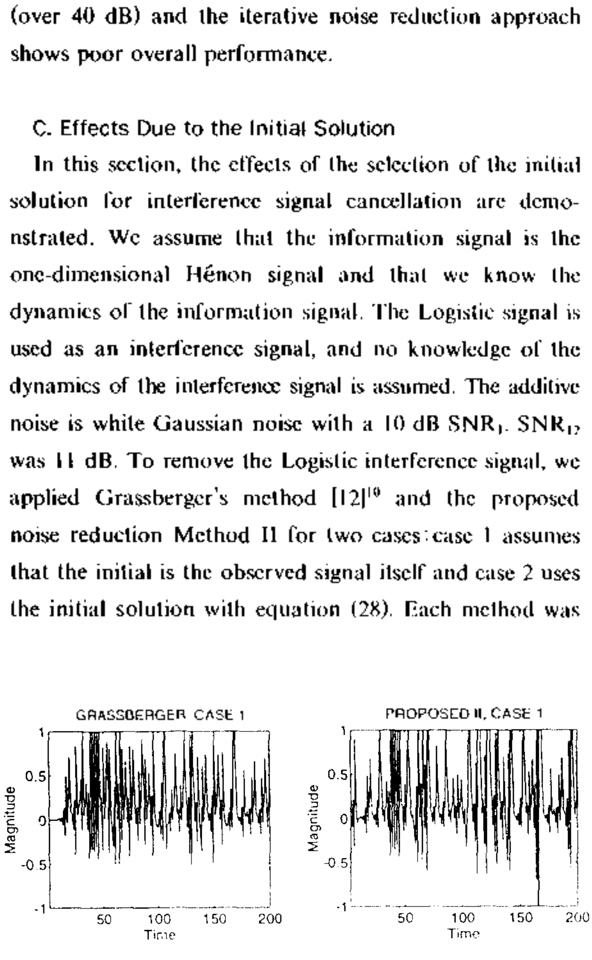

Figure 8. The true errors after applying Grassberger's method and the proposed noise reduction Method II for Case 1. The interference signal is from the Logistic system and the SNR is 10 dB.

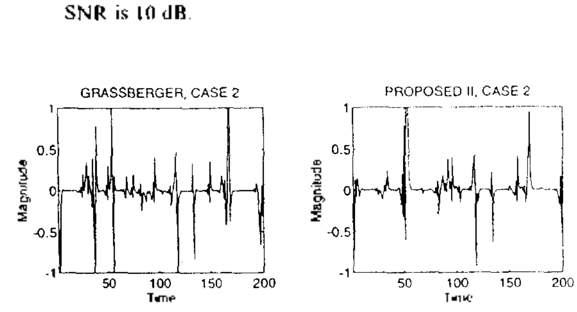

Figure 9. The true errors after applying Grassberger's method and the proposed noise reduction Method II for Case 2. The interference signal is from the Logistic system and the SNR is 10 dB.

iterated for 250 times.

Figure 8 shows the true errors of the Hénon signal after applying both methods for Case 1. Both methods failed to remove the interference Logistic signal. There are several reasons for this result. The mean value of the Logistic signal is relatively high which affects the mean value of the observed signal. Therefore, if we choose the observed signal itself as an initial solution, it is from the true solution and may lead both methods to a local minimum. On the other hand, when we choose the initial solution given by equation (28), the algorithm starts much closer to the ture solution. Figure 9 represents the true errors of the Hénon signal after applying both methods for Case 2 with the same data as for Figure 8. Both methods give good results. From these experiments, we can see that the performance of the interference signal cancellation using noise reduction methods greatly depends on the selection of the initial solution, especially, for the case when the mean value of the interference signal is much different from that of information signal.

Ⅸ. Conclusion

This paper has described a generalized iterative schemes for enhancing contaminated chaotic signals and considered their convergence conditions and error systems. The augmented system approaches are considered to separate the mixed chaotic signals under the assumption that all the system dynamics are known. Also, the interference signal cancellation problem is treated in the spirit of noise reduction and investigated for different initial solutions. Numerical experiments have been performed to compare the performance of the proposed noise reduction Methods I and II with that of Farmer's method for additive white Gaussian noise. The proposed method exhibits performance comparable to Farmer's method with the proper choice of cost functions, but has a much simpler structure. On the other hand, the proposed method requires more iterations to achieve convergence. Overall, however, the necessary computation is still less than Farmer's method because each iteration is fairly simple. For the signal separation problem, the augmented EKF approach shows good performance at high SNR_i's, while it is sensitive to noise. On the other hand, the augmented iterative noise reduction approach is not sensitive to noise, though it does not improve significantly for high SNR_i's. Also, we suggested an initial solution candidate that is especially useful for the interference signal cancellation problem. Grassberger's method and the proposed noise reduction

Method II are tested for two different initial solutions. The experiments indicate that the performance of the interference signal cancellation using reduction methods greatly depends on the selection of the initial solution.

References

1. F.C.Moon, *Chaotic and Fractal Dynamics: An Introduction for Applied Scientists and Engineers*, John Wiley & Sons, Inc., 1992.
2. T.S. Parker and L.O. Chua, "Chaos: A Tutorial for Engineers," *Proceddings of the IEEE*, vol. 75, pp 982-pp 1008, Aug. 1987.
3. S. Haykin, "Chaotic Signal Processing: New Research Dircetions and Novel Applications" *Proceedings of 6th SSAP Workshop*, pp 1-4, 1992
4. J.-P. Eckmann and D. Ruelle, "Ergodic theory of chaos and strangs attractors," *Review of Modern Physics*, vol 57, July 1985.
5. J.-P. Eckman, S.Oliffson Kamphorst, D. Ruelle, and S. Ciliberto, "Liapunov exponents from time series," *Physical Review A*, vol. 34, no. 6, pp 4971-1986.
6. K.M. Cumo and A.W. Oppenheim, "Chaotic Signals and Systems for Communications," *IEEE Proceedings of International Conference on Acoustics, Speech, and Signal Processing*, vol. 3, pp. 137-140, 1993.
7. C.W.Wu and L.O.Chua, "A simple way to synchronize chaotic with applications to secure communication systems," *International Journal of Bifurcation and Chaos*, vol. 3, no. 6, pp 1619-1627, 1993.
8. E.J. Kostelich and J.A. Yorke, "Noise reduction: Finding the simplest dynamical system consistent with the data," *Physica D* 41, pp 183-pp 196, 1990.
9. S.M. Hammel, "A noise reduction method for chaotic systems," *Physics Letters A*, vol. 148, no. 8, 9, pp 421-428, 1990.
10. J.D. Farmer and J.J. SIDdorowich, "Optimal shadowing and noise reduction," *Physica D* 47, pp. 373-392, 1991.
11. R. Cawley and J.J. SIDorowich, "Local-geometric-projection method for noise reduction in chaotic maps and flows," *Physical Review A*, vol. 46, No. 6, pp. 3057-3082, 1992.
12. P. Grassberger, R. Hegger, H. Kantz, C. Schaffrath, and T. Schreiber, "On noise reduction methods for chaotic data," *Chaos*, vol. 3, no. 2, pp. 127-141, 1993.
13. R.E. Kalman and J.E. Bertram, "Control System Analysis and Design Via the "Second Method" of Lyapunov II Discrete-Time Systems," *Journal of Basic Engineering*, vol 82, pp 394-400, June, 1960.
14. C.K Chui and G. Chen, *Kalman filtering with real-time applications*, Springer-Verlag, 1991.
15. J.E. Cohen and C.M. Newman, "The Stability of Large Random Matrices and Their Products," *The Annals of Probability*, vol. 12, no. 2, pp 283-310, 1984.
17. D.F. Drake and D.B. Williams, "Spread spectrum communications using chaotic systems," *Proceedings of the 1994 Dual Use Technologies and Applications Conference*, 1994.
18. D.F. Drake and D.B. Williams, "Tracking Multiple Chaotic Systems From A Single Observed Sequence," *Proceeding of the Sixth IEEE Digital Signal Processing Workshop*, pp. 75-78, 1994.
19. C. Lee, J. Lee, and D.B. Williams, "A Secure Communication Scheme Using Chaotic Signals," *Proc. Int. Conf. Computer Communication*, 1995

▲Chungyong Lee

Chungyong Lee received the B.S. and M.S. degrees in Electronic and Computer Engineering from Yonsei University, Seoul, Korea, in 1987 and 1989, respectively, and Ph.D. degree in Electrical and Computer Engineering from the Georgia Institute of Technology, Atlanta, GA, U.S.A., in 1995. From 1990 through 1991, he was a researcher with the Engineering Research Institute of Yonsei University. In 1996, he joined Samsung Electronic co. Ltd. as a Senior Engineer, where he has been working on speech coding and channel coding for CDMA system. His research interests include chaotic signal processing, array signal processing, and communication signal processing.

▲Douglas B. Williams

Douglas B. Williams received the B.S.E.E. (summa cum laude), the M.S., and the Ph.D. degrees in Electrical and Computer Engineering from Rice University, Houston, TX, in 1984, 1987, and 1989, respectively. In 1989, he joined the faculty of the School of Electrical and Computer Engineering at the Georgia Institute of Technology, Atlanta, research interests are in statistical signal processing with emphasis on array signal processing, non-Gaussian signal processing, and nonlinear time-series analysis.

Dr. Williams received a GE Young Faculty Award in 1990 and a NASA Graduate Student Research Fellowship for 1985~1989.

He is a member of Tau Beta Phi, Eta Kappa Nu, and Phi Beta Kappa and was an Associate Editor for the IEEE Transactions on Signal Processing.